Rare Metal Materials and Engineering
Volume 49, Issue 2, February 2020
Available online at www.rmme.ac.cn

Science Press

Cite this article as: Rare Metal Materials and Engineering, 2020, 49(2): 0454-0460.

ARTICLE

Effect of Particle Size on Microstructure and Mechanical Properties of Porous NiTi Alloys Prepared by Microwave Sintering

Xu Jilin[1], Tao Shouchen[1], Jin Xiaofei[1], Luo Junming[1], Liu Yong[2]

[1] Nanchang Hangkong University, Nanchang 330063, China; [2] Key Laboratory of Lightweight and High Strength Structural Materials of Jiangxi Province, Nanchang University, Nanchang 330031, China

Abstract: The porous NiTi alloys were prepared by microwave sintering from Ni/Ti powder with different particle sizes, and the effect of particle size on the microstructure and mechanical properties of the porous NiTi alloys was systematically investigated. The results show that the undesired Ti_2Ni and Ni_3Ti phases in the porous NiTi alloys decrease and the Ni phase disappears with decreasing the particle sizes. At the same time, the pore shapes of the porous NiTi alloys change from the irregular shape with sharp angles to the suborbicular shape. Moreover, both of the porosities and pore sizes of the porous NiTi alloys increase with increasing the particle sizes, while all of the Rockwell hardness, compressive strength and bending strength decrease. Therefore, the decrease of particle sizes is beneficial to obtain the microwave sintered porous NiTi alloys with desired microstructure (pure phase composition and uniform pore structure) and high mechanical properties.

Key words: porous NiTi alloy; microwave sintering; particle size; mechanical property; microstructure

Porous near-equiatomic nickel-titanium shape memory alloys (NiTi SMAs) have attracted considerable attentions in biomedical applications and damping applications due to their inheritance of the unique properties of dense NiTi SMAs, such as shape memory effect, superelasticity and high damping capacity[1-3]. As a biomaterial, the porous structure of NiTi alloy not only reduces the elastic modulus and avoids the stress-shielding effect, but also allows the ingrowth of new bone tissue and vascularization and obtains a firm fixation of the implants, which is potential to use in the human hard tissue repair and replacement[1,4-6]. As a damping material, the porous structure of NiTi alloy not only reduces the weight, but also further enhances the damping capacity, which has potential for use in energy-absorbing structures[2,7,8].

Since NiTi alloy has a high melting point (1310 °C), the methods for preparing porous NiTi alloy have been limited to powder metallurgy (PM) techniques[9]. Recently, many PM methods have been employed to prepare the porous NiTi alloys, including conventional sintering (CS)[10], hot isostatic pressing (HIP)[11], self-propagating high-temperature synthesis (SHS)[12], selective laser melting (SLM)[13], metal injection molding (MIM)[14], spark plasma sintering (SPS)[9,15] and microwave sintering[16,17]. Among these methods, the microwave sintering has been caused extensive research and application. Because it can utilize the microwaves directly interact with the individual particles in the green compacts and realize the rapid volumetric heating[18-20]. Compared with conventional sintering, the microwave sintering possesses many intrinsic advantages, such as reduced energy consumption, rapid heating rate, reduced sintering time, enhanced element diffusion process and improved physical and mechanical properties of the sintered materials[18-20]. It is well known that the microstructure and mechanical properties of the porous NiTi alloys mainly depend on the porosities, pore sizes and pore shapes. These pore characteristics can be adjusted through controlling the process parameters (sintering

Received date: February 18, 2019
Foundation item: National Natural Science Foundation of China (51101085, 51764041); Aeronautical Science Foundation of China (2015ZF56027, 2016ZF56020); Opening Project of Key Laboratory of Lightweight and High Strength Structural Materials of Jiangxi Province of China (20171BCD40003)
Corresponding author: Xu Jilin, Ph. D., Associate Professor, School of Materials Science and Engineering, Nanchang Hangkong University, Nanchang 330063, P. R. China, Tel: 0086-791-83863034, E-mail: jlxu@nchu.edu.cn

temperature and holding time, etc) and selecting raw powders (particle size and adding space-holder, etc). Most of the studies were focused on the effect of process parameters or adding space-holders on the pore characteristics and properties of the porous NiTi alloys[1,9-17]. To the best of our knowledge, there are few reports referred to the effect of the particle size of the raw element powders on the microstructure and mechanical properties of porous NiTi alloys. Moreover, in fact the pores formed from the original particle gaps (dependent on the particle size of the raw element powders) are difficult to alter during the sintering process, which can greatly influence the ultimate pore characteristics and mechanical properties of sintered porous materials[21]. Therefore, the present work aims to prepare the porous NiTi alloys using microwave sintering of element Ni and Ti powders, and evaluate the effect of particle sizes of Ni/Ti powders on the microstructure (porosity, pore size, pore shape and phase composition) and mechanical properties (hardness, compressive strength and bending strength) of porous NiTi alloys.

1 Experiment

Commercially available carbonyl nickel powders (purity >99.7%), electrolytic nickel powders (purity >99.7%) and dehydrided Ti powders (purity >99.9%) were used as the raw materials to prepared porous NiTi alloy. The average particle size of carbonyl nickel powders was about 2 μm. The average particle sizes of electrolytic nickel powders were 45 and 100 μm, respectively. The average particle sizes of the dehydrided Ti powders are 10, 45 and 100 μm, respectively. The SEM morphologies of the elemental powders are shown in Fig.1. The carbonyl nickel powder exhibits a near-spherical shape with some agglomerations. The electrolytic nickel powder has irregular shape with smooth surface, while the titanium powder is also irregular with sharp corners. Four kinds of Ti-50.8at%Ni blended powders were designed to investigate the effect of the particle size on the microstructure and mechanical properties of the porous NiTi alloys. The particle sizes of the blended powders are shown in Table 1. The Ti-50.8at%Ni powders were blended in a planetary ball mill (QM-3SP4, Nanjing University Instrument Plant) at speed of 200 r/min for 2 h. The blended powders were cold-pressed into green samples (6 mm×6 mm ×50 mm for bending tests and Φ20 mm×15 mm for other tests) through a uniaxial pressure of 260 MPa for 30 s. The green compact samples were sintered in a 2.45 GHz 5 kW continuously adjustable microwave equipment (NJZ4-3, Nanjing Juequan co., Ltd.) with the microwave heating at a rate of 20~30 °C/min to 1000 °C for 15 min. During the sintering process, the microwave sintering chamber was filled with high purity argon gas flow (99.999%) and a Reytek infrared pyrometer was used to measure the temperature of the sintered samples.

The pore structure of the porous NiTi alloys was investigated by an optical microscope (OM, DM1500, Shenzhen HIPOWER, China). The average pore sizes of the porous samples were analyzed by software of Nano Measurer 1.2. The general porosity (P) of the porous samples was tested by Archimedes drainage method according to ASTM B962-08[21]. The phase composition was identified by X-ray diffraction (XRD, Bruker D8 FOCUS, Germany). The surface morphologies of the green compacts and sintered samples were investigated by a field emission scanning electron microscopy (SEM, FEI Quanta 200, America). The Rockwell hardness of the porous NiTi alloys was measured by HRB-150A Hardness tester with a load of 980 N for 3 s. Compression test was carried out at ambient temperature of 25 °C with a constant rate of 0.05 mm/min on Instron WDW-50 testing machine.

Fig.1 SEM morphologies of the elemental powders: (a) carbonyl nickel, (b) electrolytic nickel (~45 μm), and (c) dehydrided Ti (~45 μm)

Table 1 Particle size of the blended powders (μm)

Sample No.	Ni powder	Ti powder
1	2	10
2	2	100
3	45	45
4	100	45

The compressive samples were machined into cylindrical solid with a dimension of Φ 5 mm×10 mm (L/D=2.0, ASTM E9-09). The bending test of the rectangular porous NiTi alloys (5 mm×5 mm×45 mm) was also carried out at ambient temperature of 25 °C with a constant rate of 0.05 mm/min on Instron WDW-50 testing machine. The bending strength (σ_f)

was calculated by the following formula:

$$\sigma_f = \frac{3FL}{2bh^2} \quad (1)$$

where F is the maximum loading during testing procedure, L is the span between two supports, and b and h represent the breadth and height of the samples, respectively. In this test, the span L was 30 mm.

2 Results and Discussion

2.1 Microstructure of the porous NiTi alloys

The OM surface morphologies of the porous NiTi alloys prepared by different particle sizes are shown in Fig.2. It can be seen that the pore sizes distributed over the surface of porous NiTi alloys increase with increasing the particle sizes, and the number of the pores increases first, and then decreases. The pores of the sample 1 exhibit isolated and suborbicular shape with the average pore size of 30.02 ±11.67 μm. The average pore size of sample 2 increases to 57.01 ±24.78 μm, while the pores are also isolated with irregular shape. Further increasing the particle sizes, the average pore size of sample 3 increases to 93.25 ±36.77 μm, and the connectivity among the pores greatly enhances. Especially, when the Ni particle size increases to 100 μm, the average pore size of the sample 4 rapidly increases to 173.98 ±77.07 μm, while the number of the pores sharply decreases compared to other samples.

The porosity values of the porous NiTi alloys prepared by the different particle sizes are shown in Fig.3. The porosities of the porous NiTi alloys increase linearly with increasing the particle sizes when the Ni particle sizes are lower than 45 μm. The porosity of sample 1 is only 22.07%, while it increases to 35.67% for the sample 3. However, as the Ni particle size increases to 100 μm, the porosity of sample 4 is 36.14%, little higher than that of sample 3. Moreover, the standard deviation of the sample 4 is much higher than other samples due to the non-uniform pore distribution.

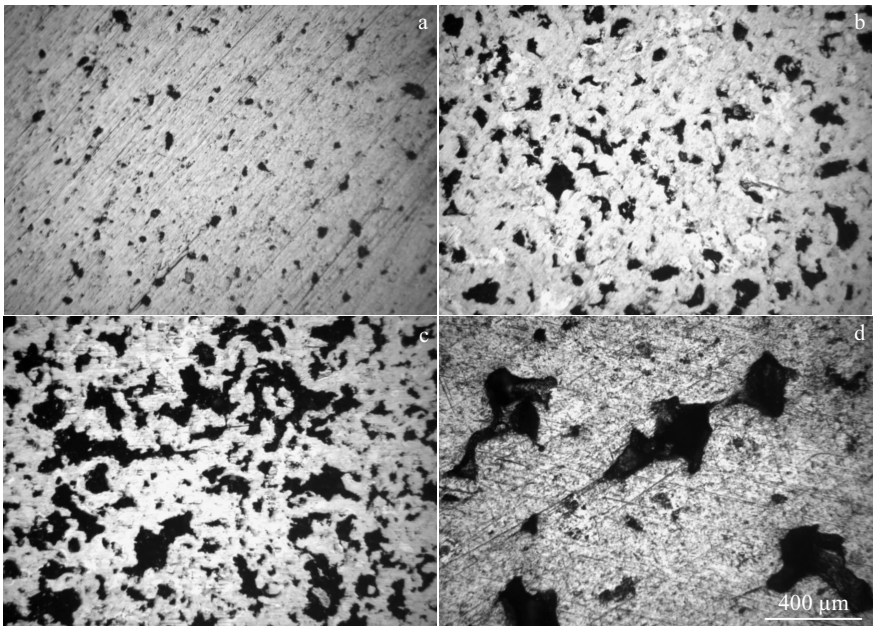

Fig.2 OM surface morphologies of the porous NiTi alloys prepared by different particle sizes: (a) sample 1, (b) sample 2, (c) sample 3, and (d) sample 4

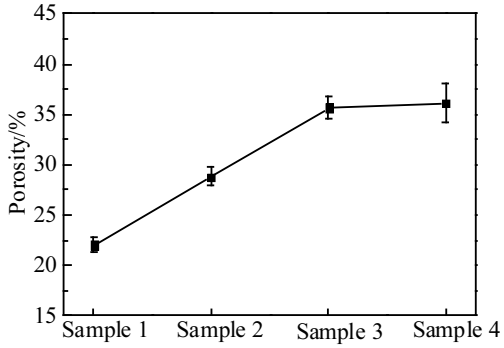

Fig.3 Porosities of the porous NiTi alloys prepared by the different particle sizes

Fig.4 shows the SEM surface morphologies of the green compacts and sintered samples. It can be seen from Fig. 4a that the large Ti particles are encircled by the fine Ni particles with many fine gaps among the particles. With increasing the particle sizes, the compact of sample 3 presents the Ni particles and the Ti particles uniformly mixed together with

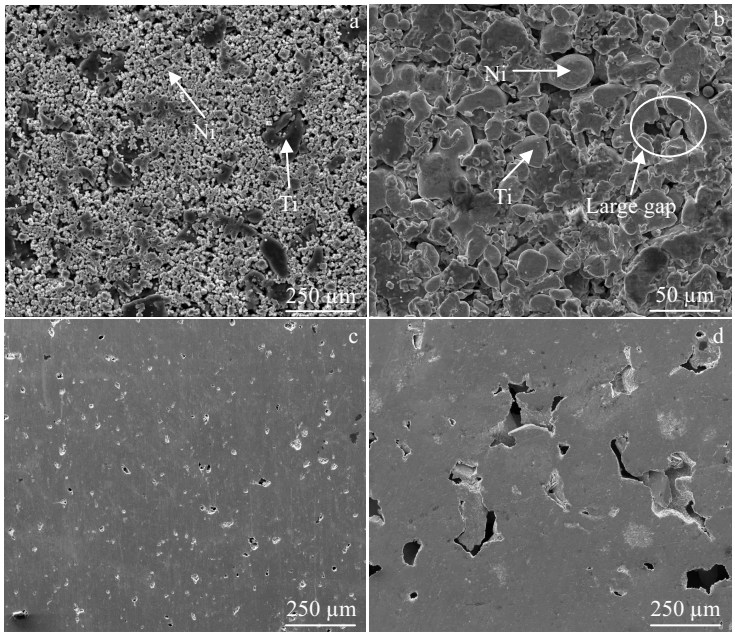

Fig.4 SEM surface morphologies of the green compact (a, b) and sintered samples (c, d): (a, c) sample 1 and (b, d) sample 3

many large irregular gaps among the particles. The gaps of the green compacts would be directly inherited to the final sintered samples, resulting in many fine quasi-circular pores distributed over the sintered sample 1 (seen in Fig. 4c) and many large irregular pores distributed over the sintered sample 3 (seen in Fig. 4d). Comparison the surface morphologies of the green compacts and the sintered samples in Fig. 4, it can be concluded that the sources and evolution of the pore structure of the sintered porous NiTi alloys with different particle sizes should be mainly resulted from the initial pores of the green compact, namely the gaps among the particles. This result is well consistent with the Ref.[21], which prepared the 316L stainless steel using the different particle sizes. Moreover, the volatilization of impurities in the green compacts, the Kirkendall effect[22,23] and the volume shrinkage during the alloying and densifying process also play roles in forming the pores.

2.2 Phase composition of the porous NiTi alloys

The XRD patterns of the porous NiTi samples prepared by the different particle sizes are shown in Fig.5. The desired B2 NiTi phase is the predominant phase in the microwave sintered porous NiTi alloys and the diffraction intensity of B2 NiTi phase decreases with increasing the particle sizes. Moreover, the diffraction peaks of Ni_3Ti, Ti_2Ni and Ni phases are obviously detected from the sample 3 and sample 4. When the particle size of Ni is 2 μm, the diffraction peaks of B2 NiTi phase obviously appear at the angles of 42.3°, 61.5° and 77.5°, respectively. When the Ni particle size is higher than 2 μm, the diffraction peaks of Ni_3Ti phase are also detected at the angles of 46.6° and 43.4°, respectively as well as the

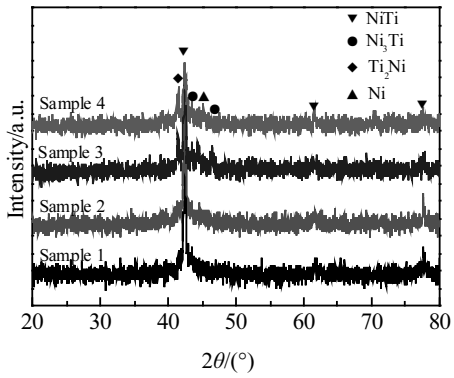

Fig.5 XRD patterns of the porous NiTi samples prepared by the different particle sizes

diffraction peak of Ti_2Ni phase at the angle of 41.4°. In addition, the diffraction peak of Ni is detected at the angle of 45.2° as the particle size of Ni reaches 100 μm.

During the microwave sintering process, the NiTi, Ti_2Ni and Ni_3Ti phases are stable compounds according to the phase diagram of the binary Ni-Ti system[23,24]. The reaction equations of the Ti and Ni are as follows[23,24]:

$$Ti+Ni \rightarrow NiTi+67\ kJ/mol \quad (2)$$

$$2Ti+Ni \rightarrow Ti_2Ni+83\ kJ/mol \quad (3)$$

$$Ti+3Ni \rightarrow Ni_3Ti+140\ kJ/mol \quad (4)$$

The formation of Ti_2Ni and Ni_3Ti phases is more thermodynamically favored according to the enthalpy of formation. While the NiTi phase can be formed as the diffusion of the Ni and Ti atoms is sufficient and the alloying

is realized completely[23].

It is also well known that the sintering process consists of alloying stage and densification stage, both of which strongly depends on the diffusion of atoms between the powder particles. The free diffusion coefficient of Ti and Ni atoms obeys to the Arrhenius equation[25]:

$$D = D_0 e^{-\frac{Q}{RT}} \quad (5)$$

where D is the diffusion coefficient, D_0 is the diffusion constant, Q is the activation energy of diffusion, R is the gas constant and T is absolute temperature. The temperature is the dominant factor in affecting the diffusion, and the higher the temperature is, the higher the diffusion coefficient obtains.

In conventional sintering, the heat transfer takes place through radiation or conduction, and the thermal energy is transferred from the sample surface to the core by conduction. However, in the microwave sintering, the whole of sample absorbs microwaves and is heated up by volumetric heating, in which the electromagnetic energy of the microwaves is converted to the thermal energy rather than heat transfer[19]. However, unlike ceramic materials, the microwave interaction with metals is restricted to its surface only. This depth of penetration in metals, also known as skin depth (δ), is defined as the distance into the material at which the incident power drops to 1/e (36.8%) of the surface value[26]. The skin depth is mathematically expressed as follows[20,26,27]:

$$\delta = \frac{1}{\sqrt{\pi f \mu \sigma}} = 0.029\sqrt{\rho \lambda_0} \quad (6)$$

where f is the microwave frequency (2.45 GHz), μ is the magnetic permeability, σ is the electrical conductivity, λ_0 is the microwave wavelength (12.24 cm) and ρ is the electrical resistivity of the metals. From Eq.(5), it is evident that most metals generally have a skin depth in the order of micrometre, which is reason for heating the metals directly using the powders with a particle size of micrometre order. Moreover, the heating efficiency and uniformity of the green compacts can enhance with deceasing the particle sizes. The skin depth of Ni particle at 500~1000 °C is 6~7 μm[27], higher than that of the carbonyl nickel powder (~2 μm) used in this paper, which can lead to its rapid heating and reach a higher diffusion coefficient, in favor of the complete alloying and formation of the NiTi phase. Especially, the diffusion of the atoms between the particles can be greatly accelerated under the microwave field, and the Ni/Ti alloying stage is also further promoted[19,28]. Moreover, the ions diffusion path increases due to the large gaps distributed over the sample 3 and sample 4, which is adverse to alloying and densification of the green compacts. Therefore, there are the reasons for that both of the sample 1 and sample 2 can obtain the relative pure NiTi phase, while the sample 3 and sample 4 contain the undesired Ti_2Ni and Ni_3Ti phases.

2.3 Mechanical properties of the porous NiTi alloys

Fig.6 shows the Rockwell hardness of the porous NiTi alloys prepared by the different particle sizes. The Rockwell hardness of the porous NiTi alloys decreases with increasing the particle sizes. The hardness of the sample 1 can reach 83.24 ±1.48 HRB, while it decreases by 24% for the sample 2 (62.88 ±1.56 HRB). Further increasing the particle sizes, the hardness of the porous NiTi alloys decreases to 38.98 ±1.09 HRB for sample 4, only 47% compared to the sample 1.

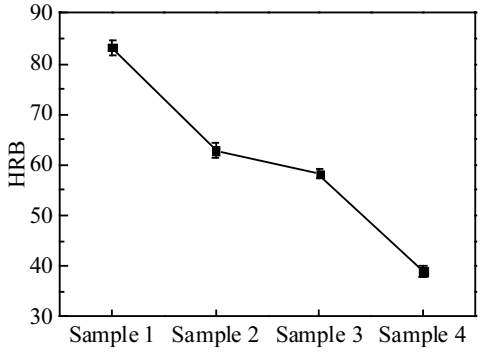

Fig.6 Rockwell hardness of the porous NiTi alloys prepared by the different particle sizes

The typical compressive stress-strain curves of the porous NiTi alloys prepared by different particle sizes are shown in Fig.7, and the compressive strength and elastic modulus of the porous NiTi alloys extracted from the stress-strain curves are shown in Fig.8. The stress-strain curves of the different samples have the same variation tendencies, which can be divided into three regions, elastic deformation region, plastic yield deformation region and densification and rupture region, consistent with Ref.[29,30]. Moreover, it is clearly seen from Fig.7 that the compressive strength and the compressive ductility of the sample 1 and sample 2 are much higher than those of sample 3 and sample 4. As shown in Fig.8, the compressive strength of the porous NiTi alloys gradually decreases with increasing the particle sizes, while the elastic modulus has a small change from 3.8±0.5 GPa to 8.1±0.9 GPa. Especially,

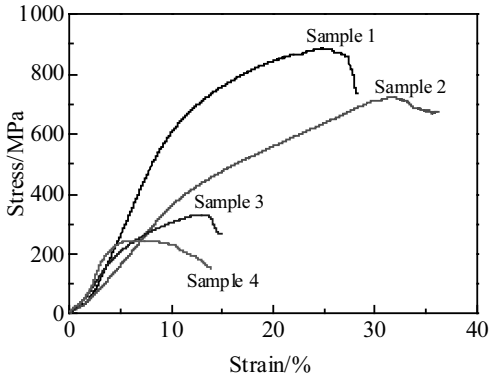

Fig.7 Typical compressive stress-strain curves of the porous NiTi alloys prepared by the different particle sizes

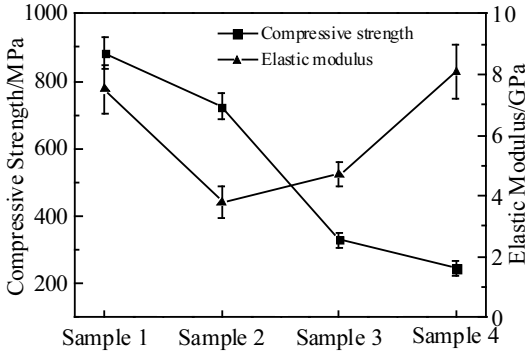

Fig.8 Compressive strength and elastic modulus of the porous NiTi alloys prepared by the different particle sizes

the compressive strength of the sample 1 can reach 882.7±45.3 MPa, nearly 4 times higher than that of sample 4.

The bending strength of the porous NiTi alloys prepared by the different particle sizes is shown in Fig.9. The bending strength of the porous NiTi alloys almost linearly decreases from 371.4±40 MPa for sample 1 to 139.3±31 MPa for sample 4 with increasing the particle sizes.

It is well known that the mechanical properties of the materials are greatly dependent on the microstructure of the materials. The particle sizes of the Ni powders and Ti powders have great effects on the porosities, pore sizes, pore shapes and phase compositions of the porous NiTi alloys, which lead to inevitably influence the mechanical properties of the porous NiTi alloys. With increasing the particle sizes, both of the porosities and pore sizes of the porous NiTi alloys increase, which results in the decrease of the support force of pore walls and inevitably deteriorates the mechanical properties (such as hardness, compressive strength and bending strength, etc.) of the samples. This result is consistent with the most of Ref. [21,29,30]. Moreover, the pores distributed over the sample 3 and sample 4 exhibit irregular with some sharp corners, which is easy to the formation of stress concentration and the further

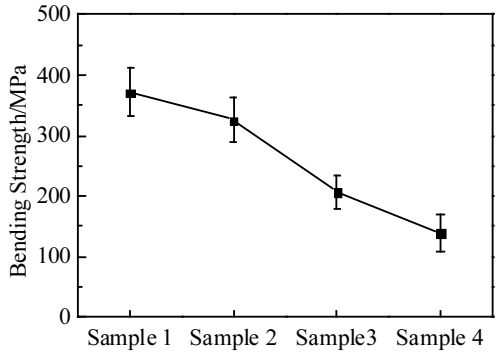

Fig.9 Bending strength of the porous NiTi alloys prepared by the different particle sizes

deterioration of mechanical properties[21,31]. The undesired second phases of Ni_3Ti and Ti_2Ni contained in the sample 3 and sample 4 are also adverse to the mechanical properties, shape memory effect and superelasticity of NiTi alloys[23,24]. There are main reasons for the decrease of the mechanical properties of porous NiTi alloys with increasing the particle sizes, especially for the dramatically reduce of sample 3 and sample 4.

According to the Ref.[6,32], the ideal load-bearing bone implant materials should have the porosity in the range of 30%~50% with the optimal pore size of 100~400 μm, and the compressive strength should be higher than 230 MPa, which is the compressive strength of the human cortical bone[33]. On the other hand, the porous NiTi alloy only possessing some specific pore structure can obtain high strength and high damping[2,7,8]. Therefore, considering the microstructure and mechanical properties of porous NiTi alloys, it can be concluded that it is unreasonable to increase the porosity of porous NiTi alloys through increasing particle sizes. Moreover, it is advisable to prepare the porous NiTi alloy using the fine Ni/Ti powders with the pore-forming agents to adjust the pore structure and porosity.

3 Conclusion

1) The porous NiTi alloys can be prepared by microwave sintering from Ni/Ti powder with different particle sizes. The pore structure of the porous NiTi alloys greatly depends on the particle sizes of Ni/Ti powders. With increasing the particle sizes, the porosities and pore sizes of the porous NiTi alloys gradually increase.

2) The porous NiTi alloy are mainly composed of the desired B2 NiTi phase with a few undesired Ti_2Ni and Ni_3Ti second phases, and the diffraction intensity of the second phases increases with increasing the particle sizes.

3) All of the Rockwell hardness, compressive strength and bending strength of the porous NiTi alloys decrease with increasing the particle sizes.

References

1 Bansiddhi A, Sargeant T D, Stupp S I *et al*. *Acta Biomaterialia*[J], 2008, 4(4): 773

2 Köhl M, Bram M, Moser A *et al*. *Materials Science and Engineering A*[J], 2011, 528(6): 2454

3 Chen Q, Thouas G A. *Materials Science and Engineering R*[J], 2015, 87: 1

4 Liu X, Wu S, Yeung K W *et al*. *Biomaterials*[J], 2011, 32(2): 330

5 Robertson D M, Pierre L, Chahal R. *Journal of Biomedical Materials Research*[J], 1976, 10(3): 335

6 Mour M, Das D, Winkler T *et al*. *Materials*[J], 2010, 3(5): 2947

7 Zhang X X, Hou H W, Wei L S *et al*. *Journal of Alloys and Compounds*[J], 2013, 550: 297

8 Guo W, Kato H. *Materials & Design*[J], 2015, 78: 74
9 Zhang L, Zhang Y Q, Jiang Y H *et al*. *Journal of Alloys and Compounds*[J], 2015, 644: 513
10 Bertheville B. *Biomaterials*[J], 2006, 27(8): 1246
11 Yuan B, Zhang X P, Chung C Y *et al*. *Materials Science and Engineering A*[J], 2006, 438-440: 585
12 Novák P, Mejzlíková L, Michalcová A *et al*. *Intermetallics*[J], 2013, 42: 85
13 Yablokova G, Speirs M, Humbeeck J V *et al*. *Powder Technology*[J], 2015, 283: 199
14 Chen G, Cao P, Wen G *et al*. *Intermetallics*[J], 2013, 37: 92
15 Zhang L, He Z Y, Tan J *et al*. *Intermetallics*[J], 2017, 82: 1
16 Tang C Y, Zhang L N, Wong C T *et al*. *Materials Science and Engineering A*[J], 2011, 528(18): 6006
17 Xu J L, Jin X F, Luo J M *et al*. *Materials Letters*[J], 2014, 124: 110
18 Das S, Mukhopadhyay A K, Datta S *et al*. *Bulletin of Materials Science*[J], 2009, 31(7): 943
19 Oghbaei M, Mirzaee O. *Journal of Alloys and Compounds*[J], 2010, 494: 175
20 Mishra R R, Sharma A K. *Composites Part A*[J], 2016, 81: 78
21 Ertugrul O, Park H S, Onel K *et al. Powder Technology*[J], 2014, 253: 703
22 Li B Y, Rong L J, Li Y Y. *Materials Science and Engineering A*[J], 2000, 281: 169
23 Hey J C, Jardine A P. *Materials Science and Engineering A*[J], 1994, 188: 291
24 Otsuka K, Ren X. *Progress in Materials Science*[J], 2005, 50(5): 511
25 Claire A D L. *Acta Metallurgica*[J], 1953, 1: 438
26 Leonelli C, Veronesi P, Denti L *et al*. *Journal of Materials Processing Technology*[J], 2008, 205: 489
27 Mondal A, Upadhyaya A, Agrawal D. *International Journal of Refractory Metals and Hard Materials*[J], 2010, 28(5): 597
28 Dube D C, Ramesh P D, Cheng J *et al*. *Applied Physics Letters*[J], 2004, 85(16): 3632
29 Gao Z, Li Q, He F *et al*. *Materials & Design*[J], 2012, 42: 13
30 Xu J L, Bao L Z, Liu A H *et al*. *Materials Science and Engineering C*[J], 2015, 46: 387
31 Li D S, Zhang Y P, Ma X *et al*. *Journal of Alloys and Compounds*[J], 2009, 474: 1
32 Yang D, Guo Z, Shao H *et al*. *Procedia Engineering*[J], 2012, 36: 160
33 Hench L L. *Journal of the American Ceramic Society*[J], 1998, 81(7): 1705

颗粒尺寸对微波烧结多孔 NiTi 合金的显微结构及力学性能的影响

徐吉林[1]，陶寿晨[1]，金晓飞[1]，罗军明[1]，刘　勇[2]

(1. 南昌航空大学，江西 南昌 330063)

(2. 南昌大学 江西省轻质高强结构材料重点实验室，江西 南昌 330031)

摘　要：以不同颗粒尺寸的 Ni/Ti 粉末为原料，采用微波烧结技术制备了多孔 NiTi 合金，并系统考察了颗粒尺寸对多孔 NiTi 合金的显微结构和力学性能的影响。结果表明，随着颗粒尺寸的减小，多孔 NiTi 合金中的 Ti_2Ni 和 Ni_3Ti 第二相减少而单质 Ni 相消失。同时，多孔 NiTi 合金的孔隙形貌由带尖角的不规则形状向近球形转变。此外，多孔 NiTi 合金的孔隙率和孔径随着颗粒尺寸的增大而增大，而洛氏硬度、抗压强度和抗弯强度均下降。因此，减小颗粒尺寸有利于获得理想的显微结构（纯净的物相和均匀的孔隙结构）和提高微波烧结多孔 NiTi 合金的力学性能。

关键词：多孔 NiTi 合金；微波烧结；颗粒尺寸；力学性能；显微结构

作者简介：徐吉林，男，1982 年生，博士，副教授，南昌航空大学材料科学与工程学院，江西 南昌 330063，电话：0791-83863034，E-mail: jlxu@nchu.edu.cm